Supplementary Materials

Materials and methods

Participants

A group of 13 observers participated in this experiment, receiving financial compensation for their time. All observers were right handed native English speakers with no history of neurological disorder. The procedure of this experiment was approved by local Institutional Review Board (IRB) committee.

Materials

The category names and category members were the same as those used in Experiment 1b of our previous behavioral study [10]. Sixteen single-word category names were selected, with twenty single-word category members for each category see Appendix 1b in (Tian & Huber, 2010). All words were displayed in upper case Times New Roman font, as yellow lettering against a black background, and subtended less than 3 degrees of visual angle. Stimulus materials were projected on a screen inside the magnetoencephalography (MEG) chamber. Two 2-button response boxes were used, with one in each hand. One button on each response box was assigned to a response.

Experimental design and procedure

The speeded category matching task used in Experiment 1b of our previous behavioral study (Tian & Huber, 2010) was replicated in this experiment. On each trial, a category name was presented above the midline for 1000 ms, followed by a category member presented below the midline while the category name remained on the screen until observers responded. Observers were asked to decide whether the category member matched or mismatched the category name. Following each response, a blank screen was presented for 500ms between trials to minimize artifacts caused by eye blinks.

A 2 (*repetition status*) X 2 (*match status*) factorial design was used, resulting in 5 repetitions of the 4 conditions across the list of 20 trials in a block. The order of these 20 trials was determined randomly. One of the 16 category names was randomly chosen without replacement to repeat on 10 trials (*repeated* condition) and 10 category names were drawn without replacement from the remaining 15 category names and were used on 10 trials (*novel* condition). In half of the trials, the category member belonged to the preceding presented category (*match* condition). The other half of trials presented a category member from a different category (*mismatch* condition). For each block, 5 category members from the repeated category were paired with 5 other category names to form *novel mismatch* trials and 5 *repeated mismatch* trials were created by pairing the repeated category name with 5 category members from 5 categories that otherwise did not appear in the block.

Sixteen blocks in which different category names served as the repeated category formed one set that used all categories equally often. All category members were randomly selected without replacement so that category members never repeated within one set. There were 3 sets such that each category served as the repeating category three times during the experiment. There were two practice blocks that used different stimuli prior to the start of the experiment. Observers were encouraged to respond as quickly and as accurately as possible.

MEG recording

Magnetic signals were measured using a 157-channel whole-head axial gradiometer system (KIT, Kanazawa, Japan). Five electromagnetic coils were attached to the observer's head prior to MEG recording to check head position within the MEG. The locations of the coils were determined with respect to three anatomical landmarks (nasion, left and right preauricular points) on the scalp using 3D digitizer software (Source Signal Imaging, Inc.) and digitizing hardware (Polhemus, Inc.). The coils were localized with respect to the MEG sensors, both at the beginning and end of the experiment.

Before the visual word experiment, observers listened to 200 repetitions of 250HZ and 1 kHz, 50 ms sinusoidal tones (ISI randomized between 750 and 1550 ms), with 100 repetitions for each frequency. Auditory-evoked responses to the onset of these pure tones were examined, and the auditory M100 was identified. The auditory M100 is a prominent and robust response, apparent around 100 ms after auditory stimuli onset and has been the most investigated auditory MEG response for review see (Roberts, Ferrari, Stufflebeam, & Poeppel, 2000). A dipole-like pattern (i.e., a source and sink pair) in the magnetic topographic map distributed over the temporal region of each hemisphere was identified for each observer. These auditory dipole patterns were used to verify whether observers were in the proper position.

The MEG data were acquired with a sampling rate of 500 Hz, filtered online between 1 Hz and 200 Hz, with a notch at 60 Hz. Raw data were noise-reduced offline using a time shift PCA method (de Cheveigné & Simon, 2007).

MEG data preprocessing

A 1000 ms time period that was time locked to the category name onset was extracted, separately for *repeated* and *novel* category names. A second 1000 ms epoch that was time locked to the category member onset was also obtained, separately for combinations of *repeated*/*novel* category names and *matching*/*mismatching* category members. Responses with amplitudes >3pT (~5%) were considered artifacts and discarded. The first trial of the *repeated* and *novel* conditions were eliminated because there was no functional difference between these conditions. The second to tenth trials in each condition were broken into thirds as a function of the number of prior repetitions (1-3, 4-6, 7-9). Epochs were determined for each third separately, and low-pass filtered with a cutoff frequency of 20 Hz.

The timing of the M100, M170, and M400 waveforms were determined separately for each individual using the root-mean-square across all sensors to the category name, collapsed across conditions. For all analyses, the M100, M170, and M400 were determined separately for each individual based on a 22 ms average centered on the appropriate delay in response to the category name, matching category member, or mismatching category member. This was done separately for all sensors and the resultant topographic patterns were used in the multivariate analyses.

Statistical analysis

Multivariate analyses

Multivariate techniques developed by Tian and Huber (Tian & Huber, 2008) were used to quantify the topographic similarity between conditions and response magnitude changes as a function of prior repetitions. The response pattern similarity was evaluated using an ‘angle test’ to infer whether the underlying neural sources distribution differed between conditions. The response topographies recorded from multiple sensors were treated as high dimensional vectors (the number of dimensions equal to the number of sensors) and the cosine of the angle between vectors in different conditions was calculated and compared to the cosine of the angle when comparing vectors from the same condition to statistically assess whether the two conditions were significantly different in terms of topographic distributions. If no differences were found, a ‘projection test’ assessed response magnitude for each condition by projecting the vector from each condition onto a standard separately defined response profile. These techniques have been found to be useful for testing psychological theories in human electrophysiological studies (Davelaar, et al., 2011; Huber, Tian, Curran, O'Reilly, & Woroch, 2008b; Tian & Huber, 2008; Tian & Poeppel, 2010) and a free toolbox for implementing these analyses is available online (Tian, et al., 2011).

The projection test of response magnitude was run as a repeated measures 2 X 3 ANOVA to check the main effect of *repeated* versus *novel* (i.e., the repetition effect), the main effect of prior repetitions broken into thirds, and the interaction between these two factors. The interaction was the key comparison, determining whether the repetition effect changed with increasing numbers of repetitions. The interaction term was checked prior to running the linear contrasts reported in the main text. However, prior to this ANOVA, we used the angle test to check whether the results of the projection test might reflect a change in the mixture of underlying neural sources, as indicated by different topographic patterns.

Angle test of topographic similarity. The experiment was divided into epochs from the first half versus epochs from the second half and the average response patterns of each half were compared to each other within the same condition (e.g., *repeated* first half versus *repeated* second half) to produce a null distribution, and between conditions (e.g., *repeated* first half versus *novel* second half) to produce an alternative distribution. For the angle test of the repetition effect, the epochs were collapsed across the number of prior repetitions. Thus, there were two within condition angle measures per individual (one for *repeated* and one for *novel*) and there were two between condition angle measures per individual (*repeated* first half versus *nonpeated* second half and *repeated* second half versus *novel* first half). The between and within condition comparisons were then averaged separately for each individual and compared across individuals with a dependent samples t-test to determine whether in general the *repeated* and *novel* conditions produced different topographic patterns. This was done separately for the M100, M170, and M400 in response to the category name, the matching category member, and the mismatching category member.

For the angle test across different numbers of prior repetitions broken into thirds, new epochs were calculated that collapsed across the *repeated* and *novel* conditions. The same first half versus second half comparisons were made in an analogous manner, except there were 3 within condition comparisons and 6 between condition comparisons that were averaged prior to the dependent samples t-tests. In the absence of any significant differences in the topographic patterns, the main effects from the projection tests, reported next, are likely due to changes in response magnitude rather than changes in the mixture of underlying neural sources. We note that it is not possible to run an angle test for the interaction between the repetition effect and numbers of prior repetitions because the angle test does not conform to a general linear model. This is because the angle measure necessarily involves pairwise comparisons rather than effects that can be summed for different manipulations. Nevertheless, the absence of any significant topographic differences for the two main effects suggests that in general the same mixture of underlying neural sources was involved in the various experimental conditions.

Projection test of response magnitude. The projection test of response magnitude requires a standard waveform that captures the processes of reading words within the context of the category matching task. This waveform should be relatively uncontaminated by other presentations that might temporally overlap. The waveform produced by the presentation of the category name satisfied these needs. Thus, a standard response for each individual was obtained by averaging responses to all presentations of category names, regardless of condition. For each individual, three different standard responses were determined to capture the M100, M170, and M400. For each condition in response to the category name, the matching category member, and the mismatching category member, the observed M100, M170, or M400 waveform was projected onto the appropriate standard response to yield a measure of response magnitude. This projection normalizes response magnitude and allows comparison across individuals [27]. These projection values were then subjected to a 2 X 3 repeated measures ANOVA examining the repetition effect (*repeated* versus *novel*), the effect of prior repetitions broken into thirds, and the interaction between these two manipulations.

Dynamic causal modeling (DCM)

DCM is a mathematical method that estimates connection efficiency between regions of interests (Friston, Harrison, & Penny, 2003). It assumes that external input induces activity perturbation only at particular specified regions (e.g. sensory) in a hierarchical neural network and that the neural activity in all areas is the results of bidirectional interaction between connected regions. The associations between different regions are modeled as an effective connection that is mathematically equivalent to the causal influence of one neural region upon another using bilinear estimation. DCM was first applied to hemodynamic responses in fMRI (Friston, et al., 2003) and later extended to event-related electrophysiological responses (David, et al., 2006) by including a 3-layer neural mass model to simulate neural activity. DCM approximates the dynamics of neural activity in sources space, which are estimated by temporally inverting a spatial forward model and by adjusting the connection strengths among the pre-determined regions of interest (Kiebel, Garrido, Moran, Chen, & Friston, 2009). Three sets of connection strength parameters are estimated: 1) external inputs to the neural system; 2) connections between regions of interest; and 3) modulation parameters that vary the connection strengths as a function of experimental manipulations.

Model specification and statistical testing. Previous studies suggest that hierarchical processes mediate reading (Bentin, et al., 1999), which at least include primary visual cortex (V1) for basic visual analysis (Tarkiainen, Helenius, Hansen, Cornelissen, & Salmelin, 1999b), a special fusiform area (visual word form area, VWFA) for abstract orthographic processing (Cohen et al., 2000b; Dehaene, Le Clec'H, Poline, Le Bihan, & Cohen, 2002b; McCandliss, et al., 2003; Nobre, et al., 1994), the middle temporal gyrus (MTG) for lexical/semantic access, and the inferior frontal gyrus (IFG) for semantic contextual integration (Lau, et al., 2008; Vigneau et al., 2006). Because high-level aspects of reading are largely left lateralized (Lau, et al., 2008; Vigneau, et al., 2006), we included six nodes (left and right V1, left and right VWFA, left MTG and left IFG) in the DCM analysis. Before analyzing the results of a particular DCM model, it is necessary to compare different DCM models that make different connectivity assumptions. There are a vast number of different possible models, but we used prior results to consider only the most plausible subset of models. For instance, there is evidence that backward connections are important for processing contextual information (Garrido et al., 2008; Kiebel, et al., 2009). Furthermore, the involvement of the right VWFA (Cohen et al., 2003) and functional difference between MTG and IFG (Lau, et al., 2008) during reading are under debate. Therefore, 24 models were constructed on the basis of three factors. The first factor was vertical bidirectionality (2 levels: either both forward and backward connections or only forward connections). The second factor was the involvement of neural regions (4 levels: all six regions, no RVWFA, no MTG, or no IFG). The third factor was the inclusion of connections between hemispheres (3 levels: bidirectional lateral connections and vertical convergence from right hemisphere onto left lateralized reading areas, vertical convergence from the right hemisphere without bidirectional lateral connections, or bidirectional lateral connections without vertical convergence from the right hemisphere). These three factors were fully crossed to form 24 models (Fig. S1).

Each region of interest (each node in DCM) was modeled as an equivalent current dipole (ECD). Dipole locations were determined using the Montreal Neurological

Institute (MNI) space (Table S6). The 24 connectivity models were compared using the category name epochs for each individual collapsed across conditions. The models were fit to each individual and Bayesian model selection was applied at the group level to determine the best model in general for all individuals (Penny, Stephan, Mechelli, & Friston, 2004). Model selection was based on the cumulative posterior log-evidence, $\ln(p(y|m))$. Log-evidence from for each individual was summed and the relative log-evidence of each model was calculated by subtracting the model with the lowest log-evidence, $\ln(p(y|m_i)) – \ln(p(y|m)_{min})$. An evidence ratio, $p(y|m_i)/p(y|m_j)$ exceeding 150 (i.e. a difference of relative log-evidence between two models larger than 5.01), suggests strong evidence (probability greater than 99%) in favor of model i (Penny, et al., 2004; Raftery, 1995). The relative log-evidence among all 24 possible models (Fig. S2A) suggested that the best model (model 13) was one that included all 6 regions with only forward vertical connections and with both lateral bidirectional connections and convergence from the right hemisphere (Fig. S2B).

Modulation effects in the different conditions were investigated for the best model (Fig. 2B), separately for the category name, matching category members, and mismatching category members. Random effects linear contrast analyses of the modulation parameters assessed whether connection efficiency differed between the *repeated* and *novel* conditions as a function of the number of prior repetitions broken into thirds. All DCM analyses were carried out using SPM8.

Supplementary text

Besides the significant linear change for the left VWFA to left MTG connection reported in the text, the repetition effect of the right V1 to right VWFA connection in response to the category name also decreased as a function of the number of prior repetitions [$t(12) = 2.42$, $p = 0.03$]. However, unlike the connection involving the MTG, this connection started from a positive value for the first third (i.e., a greater connection in the *repeated* condition) and merely returned to baseline (no difference between *repeated* and *novel*) by the final third (Table S7). Thus, it is unlikely that this connection caused the M170 and M400 to the category name to decrease in the *repeated* condition as compared to the *novel* condition and it unlikely that this connection caused observers to become slower in the *repeated* condition as compared to the *novel* condition. However, observers were faster to respond in the *repeated* condition for the first third of repetitions and this connection may have been a contributing factor to the short-term facilitation for the *repeated* condition. As seen in Tables S8-9, there were no significant linear effects for any of the connections in response to matching category members or mismatching category member, respectively.

Supplementary references

Bentin, S., Mouchetant-Rostaing, Y., Giard, M. H., Echallier, J. F., & Pernier, J. (1999). ERP Manifestations of Processing Printed Words at Different Psycholinguistic Levels: Time Course and Scalp Distribution. *Journal of Cognitive Neuroscience, 11*(3), 235-260.

Brown, C., & Hagoort, P. (1993). The processing nature of the N400: Evidence from masked priming. *Journal of Cognitive Neuroscience*, *5*(1), 34-44.

Cohen, L., Dehaene, S., Naccache, L., Lehéricy, S., Dehaene-Lambertz, G., Hénaff, M. A., & Michel, F. (2000a). The visual word form area. *Brain, 123*(2), 291.

Cohen, L., Dehaene, S., Naccache, L., Lehéricy, S., Dehaene-Lambertz, G., Hénaff, M. A., & Michel, F. (2000b). The visual word form area. *Brain, 123*(2), 291-307.

Cohen, L., Martinaud, O., Lemer, C., Lehericy, S., Samson, Y., Obadia, M., . . . Dehaene, S. (2003). Visual word recognition in the left and right hemispheres: anatomical and functional correlates of peripheral alexias. *Cerebral Cortex*, *13*(12), 1313-1333.

Davelaar, E. J., Tian, X., Weidemann, C. T., & Huber, D. E. (2011). A Habituation Account of Change Detection in same/different judgments. *Cognitive Affective & Behavioral Neuroscience*, *11*, 608-626.

David, O., Kiebel, S. J., Harrison, L. M., Mattout, J., Kilner, J. M., & Friston, K. J. (2006). Dynamic causal modeling of evoked responses in EEG and MEG. *NeuroImage, 30*(4), 1255-1272.

de Cheveigné, A., & Simon, J. Z. (2007). Denoising based on time-shift PCA. *Journal of Neuroscience Methods*, *165*(2), 297-305.

Dehaene, S., Le Clec'H, G., Poline, J. B., Le Bihan, D., & Cohen, L. (2002a). The visual word form area: A prelexical representation of visual words in the fusiform gyrus. *NeuroReport*, *13*(3), 321.

Dehaene, S., Le Clec'H, G., Poline, J. B., Le Bihan, D., & Cohen, L. (2002b). The visual word form area: A prelexical representation of visual words in the fusiform gyrus. *NeuroReport*, *13*(3), 321-325.

Fiebach, C. J., Gruber, T., & Supp, G. G. (2005). Neuronal mechanisms of repetition priming in occipitotemporal cortex: spatiotemporal evidence from functional magnetic resonance imaging and electroencephalography. *The Journal of neuroscience, 25*(13), 3414-3422.

Francis, G., Grossberg, S., & Mingolla, E. (1994). Cortical dynamics of feature binding and reset: Control of visual persistence. *Vision Research, 34*(8), 1089-1104.

Friston, K. J., Harrison, L., & Penny, W. (2003). Dynamic causal modelling. *NeuroImage, 19*(4), 1273-1302.

Garrido, M. I., Friston, K. J., Kiebel, S. J., Stephan, K. E., Baldeweg, T., & Kilner, J. M. (2008). The functional anatomy of the MMN: A DCM study of the roving paradigm. *NeuroImage, 42*(2), 936-944.

Garrido, M. I., Kilner, J. M., Kiebel, S. J., & Friston, K. J. (2009). Dynamic causal modeling of the response to frequency deviants. *Journal of Neurophysiology, 101*(5), 2620-2631.

Grossberg, S. (1969). On the production and release of chemical transmitters and related topics in cellular control. *Journal of Theoretical Biology, 22*(2), 325-364.

Grossberg, S., & Myers, C. W. (2000). The resonant dynamics of speech perception: Interword integration and duration-dependent backward effects. *Psychological Review, 107*(4), 735-767.

Halgren, E., Dhond, R. P., Christensen, N., Van Petten, C., Marinkovic, K., Lewine, J. D., & Dale, A. M. (2002). N400-like magnetoencephalography responses modulated by semantic context, word frequency, and lexical class in sentences. *Neuroimage, 17*(3), 1101-1116.

Hubel, D. H., & Wiesel, T. N. (1962). Receptive fields, binocular interaction and functional architecture in the cat's visual cortex. *Journal of physiology, 160*(1), 106.

Huber, D. E., Tian, X., Curran, T., O'Reilly, R. C., & Woroch, B. (2008a). The dynamics of integration and separation: ERP, MEG, and neural network studies of immediate repetition effects. *Journal of Experimental Psychology: Human Perception and Performance, 34*(6), 1389.

Huber, D. E., Tian, X., Curran, T., O'Reilly, R. C., & Woroch, B. (2008b). The dynamics of integration and separation: ERP, MEG, and neural network studies of immediate repetition effects. *Journal of Experimental Psychology: Human Perception and Performance, 34*(6), 1389-1416.

Kiebel, S. J., Garrido, M. I., Moran, R., Chen, C. C., & Friston, K. J. (2009). Dynamic causal modeling for EEG and MEG. *Human brain mapping, 30*(6), 1866-1876.

Kutas, M., & Federmeier, K. D. (2000). Electrophysiology reveals semantic memory use in language comprehension. *Trends in Cognitive Sciences, 4*(12), 463-469.

Kutas, M., & Hillyard, S. A. (1980). Reading senseless sentences: brain potentials reflect semantic incongruity. *Science, 207*(4427), 203-205.

Lambert, W. E., & Jakobovits, L. A. (1960). Verbal satiation and changes in the intensity of meaning. *Journal of Experimental Psychology, 60*(6), 376-383.

Landauer, T. K., & Dumais, S. T. (1997). A solution to Plato's problem: The latent semantic analysis theory of acquisition, induction, and representation of knowledge. *Psychological Review; Psychological Review, 104*(2), 211.

Lau, E. F., Phillips, C., & Poeppel, D. (2008). A cortical network for semantics:(de) constructing the N400. *Nature Reviews Neuroscience, 9*(12), 920-933.

McCandliss, B. D., Cohen, L., & Dehaene, S. (2003). The visual word form area: expertise for reading in the fusiform gyrus. *Trends in Cognitive Sciences, 7*(7), 293-299.

Morewedge, C. K., Huh, Y. E., & Vosgerau, J. (2010). Thought for Food: Imagined Consumption Reduces Actual Consumption. *Science, 330*(6010), 1530-1533. doi: 10.1126/science.1195701

Nobre, A. C., Allison, T., & McCarthy, G. (1994). Word recognition in the human inferior temporal lobe. *Nature, 372*(6503), 260-263.

O'Regan, J. K., Rensink, R. A., & Clark, J. J. (1999). Change-blindness as a result of ‘mudsplashes’. *Nature, 398*(6722), 34-34.

Penny, W., Stephan, K., Mechelli, A., & Friston, K. (2004). Comparing dynamic causal models. *NeuroImage, 22*(3), 1157-1172.

Raftery, A. E. (1995). Bayesian model selection in social research. *Sociological methodology, 25*, 111-164.

Roberts, T. P. L., Ferrari, P., Stufflebeam, S. M., & Poeppel, D. (2000). Latency of the auditory evoked neuromagnetic field components: stimulus dependence and insights toward perception. *J Clin Neurophysiol, 17*(2), 114-129.

Severance, E., & Washburn, M. F. (1907). Minor studies from the psychological laboratory of Vassar College: The loss of associative power in words after long fixation. *American Journal of Psychology, 18*(2), 182-186.

Tarkiainen, A., Helenius, P., Hansen, P. C., Cornelissen, P. L., & Salmelin, R. (1999a). Dynamics of letter string perception in the human occipitotemporal cortex. *Brain, 122*(11), 2119.

Tarkiainen, A., Helenius, P., Hansen, P. C., Cornelissen, P. L., & Salmelin, R. (1999b). Dynamics of letter string perception in the human occipitotemporal cortex. *Brain, 122*(11), 2119-2132.

Thomson, A. M. (1997). Activity dependent properties of synaptic transmission at two classes of connections made by rat neocortical pyramidal axons in vitro. *Journal of physiology, 502*(1), 131-147.

Tian, X., & Huber, D. E. (2008). Measures of Spatial Similarity and Response Magnitude in MEG and Scalp EEG. *Brain Topography, 20*(3), 131-141.

Tian, X., & Huber, D. E. (2010). Testing an associative account of semantic satiation. *Cognitive Psychology, 60*(4), 267-290.

Tian, X., & Poeppel, D. (2010). Mental Imagery of Speech and Movement Implicates the Dynamics of Internal Forward Models. *Frontiers in Psychology, 1*(166). Retrieved from doi:10.3389/fpsyg.2010.00166

Tian, X., Poeppel, D., & Huber, D. E. (2011). TopoToolbox: using sensor topography to calculate psychologically meaningful measures from event-related EEG/MEG. *Computational intelligence and neuroscience, 2011*. Retrieved from doi:10.1155/2011/674605

Tsodyks, M. V., & Markram, H. (1997). The neural code between neocortical pyramidal neurons depends on neurotransmitter release probability. *Proceedings of the National Academy of Sciences of the United States of America, 94*(2), 719.

Vigneau, M., Beaucousin, V., Herve, P. Y., Duffau, H., Crivello, F., Houde, O., . . . Tzourio-Mazoyer, N. (2006). Meta-analyzing left hemisphere language areas: phonology, semantics, and sentence processing. *NeuroImage, 30*(4), 1414-1432.

Supplementary tables

Table S1. Angle tests comparing *repeated* and *novel* conditions

	Category name		Matching category member		Mismatching category member	
	t(12)	*p*	*t*(12)	*p*	*t*(12)	*p*
M100	-0.79	0.45	0.18	0.86	2.10	0.06
M170	0.95	0.36	1.56	0.15	0.82	0.43
M400	1.78	0.10	-0.72	0.48	1.54	0.15

Table S2. Angle tests comparing different numbers of prior repetitions

	Category name		Matching category member		Mismatching category member	
	t(12)	*p*	*t*(12)	*p*	*t*(12)	*p*
M100	0.90	0.38	1.50	0.46	1.09	0.30
M170	1.80	0.10	1.92	0.08	1.56	0.15
M400	0.99	0.34	1.63	0.13	1.75	0.11

Table S3. Projection tests in response to the category name.

	Main effect (*repeated* vs. *novel*)		Main effect (number of prior repetitions)		Interaction	
	F(1,12)	*p*	*F*(2,24)	*p*	*F*(2,24)	*p*
M100	0.01	0.93	0.37	0.70	0.27	0.77
M170	6.07	0.03	2.63	0.09	4.33	0.03
M400	3.10	0.10	1.38	0.27	4.35	0.02

Table S4. Projection tests in response to matching category members

	Main effect (*repeated* vs. *novel*)		Main effect (number of prior repetitions)		Interaction	
	F(1,12)	*p*	*F*(2,24)	*p*	*F*(2,24)	*p*
M100	0.00	0.98	0.89	0.43	0.76	0.48
M170	0.50	0.49	0.51	0.61	0.63	0.54
M400	0.77	0.40	0.22	0.80	3.74	0.04

Table S5. Projection tests in response to mismatching category members

	Main effect (*repeated* vs. *novel*)		Main effect (number of prior repetitions)		Interaction	
	F(1,12)	*p*	*F*(2,24)	*p*	*F*(2,24)	*p*
M100	0.90	0.36	0.54	0.59	0.36	0.70
M170	3.23	0.10	0.88	0.43	0.14	0.87
M400	5.49	0.04	1.42	0.26	0.11	0.90

Table S6. Location of equivalent current dipoles according to MNI space (mm).

Left primary visual cortex (LV1)	-20, -95, -5
Right primary visual cortex (RV1)	20, -95, -5
Left visual word form area (LVWFA)	-48, -56, -18
Right visual word form area (RVWFA)	48,-56, -18
Left middle temporal gyrus (LMTG)	-59, -37, -5
Right middle temporal gyrus (LIFG)	-44, 20, 5

Table S7. Average modulation parameter differences (*repeated* minus *novel*) and linear contrast results in response to category names as a function of prior repetitions. Abbreviation is the same as in Table S6.

	1-3	4-6	7-9	Linear contrast (p values)
LV1 → LVWFA	-0.177	-0.068	-0.019	0.21
RV1 → RVWFA	0.319	-0.052	-0.050	0.03
LVWFA → LMTG	0.030	-0.218	-0.446	0.03
RVWFA → LMTG	-0.239	0.073	-0.133	0.62
LMTG → LIFG	0.027	-0.124	-0.051	0.73

Table S8. Average modulation parameter differences (*repeated* minus *novel*) and linear contrast results in response to matching category members as a function of prior repetitions. Abbreviation is the same as in Table S6.

	1-3	4-6	7-9	Linear contrast (p values)
LV1 → LVWFA	0.185	-0.077	-0.006	0.28
RV1 → RVWFA	-0.090	-0.098	-0.082	0.95
LVWFA → LMTG	-0.313	0.184	-0.182	0.43
RVWFA → LMTG	-0.066	-0.112	-0.076	0.97
LMTG → LIFG	0.034	0.142	0.119	0.65

Table S9. Average modulation parameter differences (*repeated* minus *novel*) and linear contrast results in response to mismatching category members as a function of prior repetitions. Abbreviation is the same as in Table S6.

	1-3	4-6	7-9	Linear contrast (p values)
LV1 → LVWFA	-0.123	-0.136	0.124	0.25
RV1 → RVWFA	-0.172	-0.042	0.015	0.25
LVWFA → LMTG	-0.003	0.133	-0.161	0.60
RVWFA → LMTG	0.138	0.013	-0.189	0.08
LMTG → LIFG	-0.069	0.001	-0.043	0.86

Supplementary figure captions

Fig. S1. Twenty-four connectivity models tested with DCM. Acronyms: V1: primary visual cortex; VWFA: visual word form area; MTG: middle temporal gyrus; IFG: inferior frontal gyrus.

Fig. S2. DCM Bayesian model selection results. (A) Relative log-evidence of all 24 models (numbers labeled as in Fig. S1). (B) The posterior probability from model selection.

Fig. S1

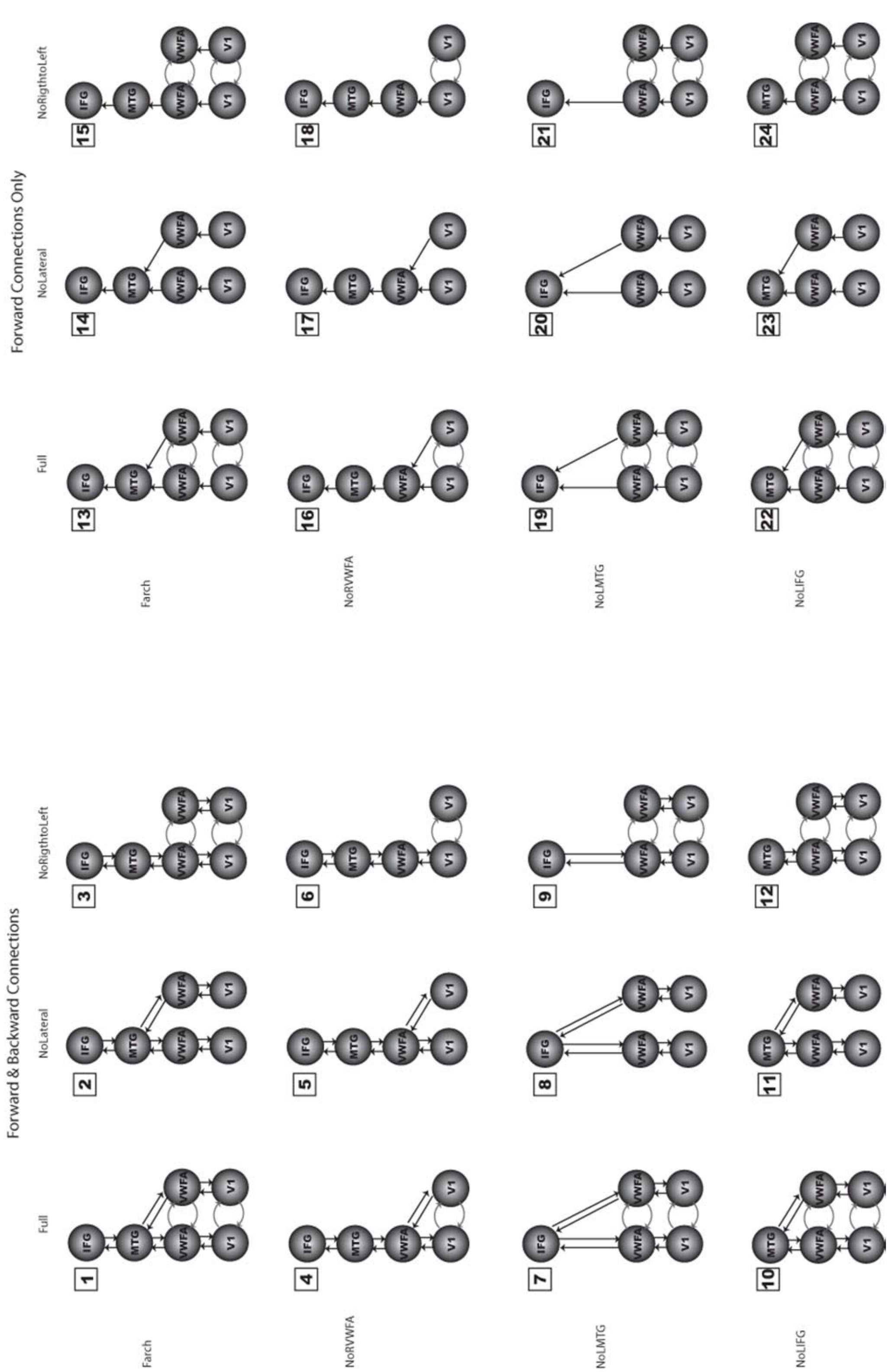

Forward & Backward Connections
Forward Connections Only
Full
NoLateral
NoRigthtoLeft
Farch
NoRVWFA
NoLMTG
NoLIFG
1
2
3
4
5
6
7
8
9
10
11
12
13
14
15
16
17
18
19
20
21
22
23
24
IFG
MTG
VWFA
V1

Fig. S2

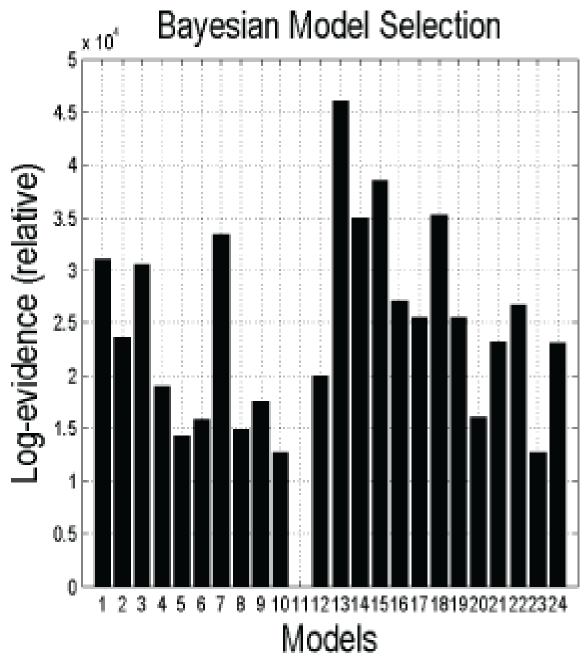
Bayesian Model Selection
x 10^4
Log-evidence (relative)
0
0.5
1
1.5
2
2.5
3
3.5
4
4.5
5
1 2 3 4 5 6 7 8 9 10 11 12 13 14 15 16 17 18 19 20 21 22 23 24
Models

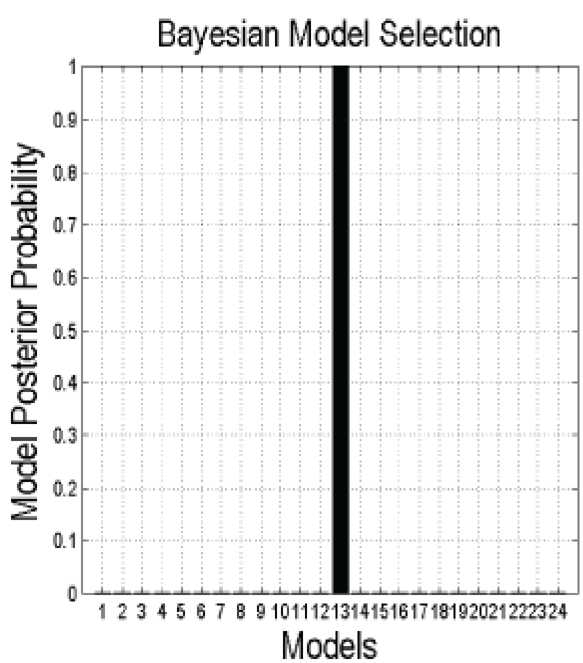
Bayesian Model Selection
Model Posterior Probability
0
0.1
0.2
0.3
0.4
0.5
0.6
0.7
0.8
0.9
1
1 2 3 4 5 6 7 8 9 10 11 12 13 14 15 16 17 18 19 20 21 22 23 24
Models